Accurate Beam Training for RIS-Assisted Wideband Terahertz Communication

Yuhao Chen, *Graduate Student Member, IEEE*, Jingbo Tan, *Member, IEEE*, Mo Hao,
Richard MacKenzie, and Linglong Dai, *Fellow, IEEE*

Abstract— **Terahertz (THz) communications have been widely considered as one of the promising technologies for future 6G wireless systems. In order to cope with the high path loss in THz systems, reconfigurable intelligent surface (RIS) composed of low-complexity reflecting elements can be deployed to generate directional beams. In order to acquire the direction of user equipment (UE) to send directional beams, the acquisition of accurate channel state information (CSI) is very important. Beam training is widely utilized to acquire the CSI. However, existing beam training schemes have not taken the wideband beam split effect into consideration, so the beam training accuracy decreases a lot in wideband scenarios. To solve this problem, in this paper, we propose an analytical beam training framework in RIS-assisted wideband THz communication systems. Specifically, we first propose a power distribution pattern (PDP) based direction estimation scheme, where the exact value of the received power is utilized to analytically calculate the UE direction. Then, we design the analytical codebook for the proposed framework based on the inherent parameters of the wideband THz system. Simulation results show that the proposed framework can achieve the near-optimal achievable rate performance with a lower beam training overhead than existing schemes.**

Index Terms— **Terahertz communication, reconfigurable intelligent surface, beam training, wide beam.**

I. INTRODUCTION

TERAHERTZ (THz) communication is considered as one of the promising technologies to satisfy the high data rate requirement for future 6G systems. It is capable of providing tens of GHz of bandwidth, which is much wider than the bandwidth that millimeter communication can provide for 5G systems [1], [2], [3], [4]. However, due to the high frequency of THz band, the THz signals suffer from

a severe path loss [5], which limits the coverage of THz signals. Moreover, significant attenuation happens when THz signals are blocked by obstacles such as buildings and trees. Fortunately, reconfigurable intelligent surface (RIS) has been proposed to overcome the above two problems [6], [7], [8], [9], [10]. A RIS is composed of numerous low-cost reflecting elements, each of which can reflect the incident signal with a particularly designed phase shift or amplitude. The THz RIS can be realized based on metal-oxide-semiconductor-based chip tiles or electron gas structure [11], [12]. By designing the *frequency-independent* phase shift of each element, a directional beam with high array gain can be generated to overcome the high path loss of THz signals. In addition, deploying RIS in communication systems can provide extra reflecting paths to solve the blockage problem when the line-of-sight (LoS) path from base station (BS) to user equipment (UE) is blocked, even if the phase estimation is inaccurate [13], [14], [15], [16], [17].

In RIS-assisted communication systems, accurate channel state information (CSI) is required to realize accurate beamforming. The CSI can be obtained either by explicit channel estimation or by implicit beam training. Due to the massive reflecting units needed to realize high array gain in RIS-assisted THz systems, the dimension of the channel is usually high. Thus, traditional channel estimation schemes suffer from an unacceptable pilot overhead in RIS-assisted THz systems [7]. To avoid obtaining the full CSI with high dimension, various implicit beam training schemes have been designed to realize the near-optimal achievable rate performance without knowing the full CSI [18], [19], [20], [21]. In beam training, a codebook that consists of codewords corresponding to different physical directions in space is designed at first. Then, the codewords in the designed codebook are sequentially transmitted to search the whole space to obtain partial CSI. The partial CSI contains the information of the physical direction of UE, which is decided by the codeword with the maximum received power. Therefore, the achievable data rate performance only decreases slightly by transmitting pencil beams to the UE direction [22].

A. Prior Works

Beam training has been widely studied in massive multiple-input multiple-output (MIMO) systems and RIS-assisted systems. A natural beam training scheme is to exhaustively search all possible directions in space [23]. Specifically, a discrete Fourier transform (DFT) codebook consisting of a set

of narrow beams was pre-designed to cover the whole space. After the training stage, the UE direction can be decided by selecting the codeword with the maximum received power.

Unfortunately, as the number of antenna elements increases, the number of candidate beams increases, and the beam training overhead increases accordingly. To cope with this problem, several schemes have been proposed. One typical solution is hierarchical search [24], [25], [26], [27]. In hierarchical search, lower-layer codebooks consist of wider beams than higher-layer codebooks. Accordingly, higher-layer codebooks have a higher angular resolution than lower-layer codebooks. For each layer, the beam with the maximum received power is chosen, and which higher-layer codebook should be utilized in the next layer is then decided. The searching range reduces and the angular resolution improves as the layer becomes high. The UE direction is finally decided after finishing the highest-layer search. By hierarchical search, the beam training overhead can be largely reduced, since wrong directions are excluded in the lower-layer steps, which avoids a large amount of unnecessary high-resolution search. However, the hierarchical search requires frequent feedback from the user to the BS/RIS, which introduces an extra burden to the communication systems. In addition, the hierarchical search is hard to be extended to multi-user scenarios, since individual interaction between each user and the BS/RIS is needed during the training process.

Another solution can handle the above two problems properly with a low beam training overhead, which simultaneously searches multiple directions in space by generating multi-directional beams [21], [28]. Specifically, the whole space is divided into several disjoint subsets, each of which contains several directions. During the searching procedure, in each time slot, a multi-directional beam is generated to search several directions corresponding to a certain subset. After a round of scanning, the subset containing the UE direction is selected according to the maximum received power. Then, to identify the exact UE direction, a few more rounds of scanning need to be conducted. In each round, the directions contained in each subset are randomized and the subsets which are corresponding to the maximum received power are recorded. The UE direction is finally determined according to the intersection of the recorded subsets. By multi-directional search, the whole space is explored in a more efficient way, since several directions can be simultaneously detected in one time slot. Thus, the beam training overhead can be significantly reduced. In addition, this scheme avoids frequent interaction between the UE and BS/RIS, which makes it easier to be extended to multi-user scenarios. In addition, data-driven based schemes can be utilized to reduce the beam training overhead [29], [30], which also avoid the frequent interaction between the UE and BS/RIS.

However, existing schemes above will suffer from severe performance degradation in wideband RIS-assisted THz systems. The reason is that the beam split effect makes it impossible to generate directional beams with high angular resolution, which are the foundation of accurate beam training. Specifically, beam split means that the beams will split into totally different physical directions over different subcarriers due to the large bandwidth and the narrow beam width [31],

[32], [33], [34]. As a consequence, only the subcarriers whose frequency are close to the central frequency can be steered to the target UE direction, while most subcarriers are steered to other directions. That is to say, the angular resolution of the generated beams decreases a lot compared to that of narrowband systems. Some hardware modules such as time-delayers can be introduced into the precoding structure to provide *frequency-dependent* phase shifts [34], [35], [36], [37], [38], thus generating beams with high angular resolution. Therefore, in wideband massive MIMO systems, the beam training accuracy of the above schemes is still high. Nevertheless, as has been mentioned above, due to the hardware limitation, RIS can only provide *frequency-independent* phase shifts for all subcarriers, making beam split effect an inevitable problem in RIS-assisted wideband THz systems. To the best of our knowledge, how to eliminate the consequence brought by the beam split effect so as to improve the accuracy of beam training in RIS-assisted wideband systems has not been studied.

B. Our Contributions

To fill in this gap, we take advantage of the beam split effect in RIS-assisted wideband THz systems to realize an accurate beam training. We reveal that the beam split effect in wideband systems makes the received power of a certain beam varies in a particular power distribution pattern (PDP), which actually carries the information of different directions in space. This new observation inspires us that, unlike the traditional way to estimate the UE direction by selecting the angle corresponding to the codeword which has the maximum received power, we can instead exploit the PDP to analytically calculate the UE direction[1]. The specific contributions of this paper are summarized as follows.

- We propose an analytical beam training framework for RIS-assisted wideband THz communication systems. In wideband THz systems, the beam split effect causes the beam at different subcarriers to split into totally different physical angles. This means that the received powers at different directions vary in a particular PDP, which contains the information of different UE directions in space. Therefore, we abandon the traditional way of selecting the beam which has the maximum received power, since the accuracy of the estimated direction decreases due to the low angular resolution caused by the beam split effect. Instead, we exploit the PDP at different physical directions to analytically calculate the UE direction based on the value of the received power.

- Based on the proposed framework, we then elaborate the analysis of the PDP at different physical angles for a certain beam, which is related to the central frequency and the bandwidth of the THz system. Then, to eliminate the difference of received powers brought by different distances, we design a beam pair for further analysis. The beam pair consists of two beams with the same width, which are adjacent to each other. A ratio metric based

---

[1]Simulation codes are provided to reproduce the results in this paper: http://oa.ee.tsinghua.edu.cn/dailinglong/publications/publications.html.

on the respective received powers of the beam pair is then introduced. The analysis shows that the ratio metric and the physical direction in space are in one-to-one correspondence. Therefore, we can analytically estimate the UE direction by the exact value of the received powers of the beam pair.

- Based on the above PDP analysis, we design a codebook for the proposed analytical beam training framework. This codebook is designed based on the inherent parameters of the wideband THz systems such as the central frequency and the bandwidth. During the beam training stage, the codewords in the designed codebook are transmitted sequentially, and the UE direction can be then estimated based on the exact values of the received power of different beam pairs. Finally, simulation results are provided to validate the proposed analytical beam training framework, which reveals that the proposed framework can realize more accurate beam training and achieve a higher data rate than existing schemes in RIS-assisted wideband THz systems.

C. Organization and Notation

The remainder of this paper is organized as follows. In Section II, we first introduce the system model of RIS-assisted wideband THz communication systems. Then, we introduce the traditional beam training framework based on DFT codebook. In Section III, we first introduce the proposed analytical beam training framework. Then we elaborate the analysis of the PDP in the wideband THz systems and introduce the corresponding PDP-based direction estimation scheme, based on which we design the codebook for the proposed analytical beam training framework. Section IV shows the simulation results. Finally, conclusions are drawn in Section V.

Notation: Lower-case and upper-case boldface letters represent vectors and matrices, respectively; $(\cdot)^T, (\cdot)^H$ denote the transpose and conjugate transpose, respectively; $\|\cdot\|_k$ denotes the k-norm of a matrix; $|\cdot|$ denotes the absolute operator; $\mathbf{v}[i]$ denotes the i-th element of a vector; $\mathbf{M}[:,i]$ denotes the i-th column of a matrix, $\mathcal{CN}(\boldsymbol{\mu}, \boldsymbol{\Sigma})$ denotes the Gaussian distribution with mean $\boldsymbol{\mu}$ and covariance $\boldsymbol{\Sigma}$; $\mathcal{U}(a,b)$ denotes the uniform distribution between a and b.

II. SYSTEM MODEL AND BACKGROUND

In this section, we first introduce the system model of the RIS-assisted wideband THz communication system. Then, the traditional beam training framework based on DFT codebook is reviewed.

A. System Model

We consider a downlink RIS-assisted wideband THz communication system, as illustrated in Fig. 1, where both the BS and the UE are equipped with a single antenna, and the RIS is an N-element uniform linear array (ULA). Thanks to the high array gain brought by RIS, the coverage of THz signals can be extended and the proposed schemes can be utilized in various communication scenarios. The BS uses orthogonal
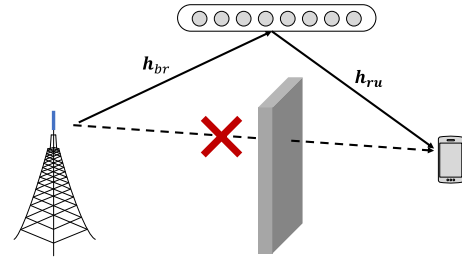

Fig. 1. RIS-assisted wideband THz communication system.

frequency division multiplexing (OFDM) with M subcarriers to serve the UE. The bandwidth of the system is denoted as B.

We considered the ray-based channel model for wideband THz channel [39]. Due to the severe loss incurred by the scattering, THz communication heavily relies on the LoS path [22], so we only consider the LoS path in this paper. Specifically, the downlink channel at the m-th subcarrier between the BS and the RIS $\mathbf{h}_{br,m} \in \mathbb{C}^{N \times 1}$ with $m = 1, 2, \cdots, M$ can be denoted as

$$\mathbf{h}_{br,m} = g_{br,m} e^{-j2\pi\tau_{br,m}f_m} \mathbf{a}_N(\varphi_m), \qquad (1)$$

where $g_{br,m}$ and $\tau_{br,m}$ denote the path gain and the time delay, respectively, f_m denotes the frequency of the m-th subcarrier, which satisfies $f_m = f_c + \frac{B}{M}\left(m - 1 - \frac{M-1}{2}\right)$ with f_c being the central carrier frequency of the system, and $\mathbf{a}_N \in \mathbb{C}^{N \times 1}$ denotes the array response vector which satisfies

$$\mathbf{a}_N(\varphi_m) = \frac{1}{\sqrt{N}}\left[1, e^{j\pi\varphi_m}, e^{2j\pi\varphi_m}, \cdots, e^{(N-1)j\pi\varphi_m}\right]^T, \qquad (2)$$

where φ_m denotes the spatial angle, which satisfies $\varphi_m = \frac{2d}{c}f_m \sin(\gamma)$ with γ being the physical angle, d is the antenna spacing, and c is the speed of light.

Similar to the definition of $\mathbf{h}_{br,m}$, the downlink channel at the m-th subcarrier between the RIS and the UE $\mathbf{h}_{ru,m} \in \mathbb{C}^{N \times 1}$ with $m = 1, 2, \cdots, M$ can be denoted as

$$\mathbf{h}_{ru,m} = g_{ru,m} e^{-j2\pi\tau_{ru,m}f_m} \mathbf{a}_N(\psi_m), \qquad (3)$$

where $g_{ru,m}, \tau_{br,m}, f_m$, and ψ_m denote the path gain, the time delay, the frequency of the m-th subcarrier, and the spatial angle, respectively. The spatial angle ψ_m satisfies $\psi_m = \frac{2d}{c}f_m \sin(\varsigma)$, where ς is the physical angle of the UE. In the following sections, we denote $\phi = \sin(\varsigma)$ for brevity.

According to (1) and (3), the channels in wideband THz systems are dependent on the frequencies of subcarriers. On the contrary, for the RIS, each of the elements can reflect the incident signal with a frequency-independent phase shift [40]. This mismatch makes the beams at different subcarriers split into different directions. Let θ_n and β_n denote the phase shift and the amplitude of the reflection coefficient of the n-th RIS element, respectively. The phase shift matrix $\boldsymbol{\Theta}$ of the RIS can be presented as

$$\boldsymbol{\Theta} \triangleq \operatorname{diag}\left(\beta_1 e^{j\theta_1}, \beta_2 e^{j\theta_2}, \cdots, \beta_N e^{j\theta_N}\right), \qquad (4)$$

where $\theta_n \in [0, 2\pi)$ and $\beta_n \in [0, 1]$ for all $n = 1, 2, \cdots, N$. Eq. (4) reveals that the electromagnetic response of all the RIS elements is frequency-independent. For simplicity, we assume the phase can be shifted continuously, and $\beta_n = 1$ for all $n \in \{1, 2, \cdots, N\}$.

Based on the channel model and the phase-shift matrix mentioned above, the received signal y_m at the m-th subcarrier at the UE can be presented as

$$y_m = \mathbf{h}_{ru,m}^H \boldsymbol{\Theta} \mathbf{h}_{br,m} s_m + n_m, \tag{5}$$

where $\mathbf{h}_{ru,m}, \boldsymbol{\Theta}$, and $\mathbf{h}_{br,m}$ denote the channel between RIS and UE, the phase-shift matrix of RIS, and the channel between BS and RIS, respectively. s_m denotes the transmitted signal at the m-th subcarrier, and n_m is the AWGN noise at the m-th subcarrier obeying a Gaussian distribution $\mathcal{CN}(0, \sigma^2)$ with noise power σ^2. We consider the scenario where the direct link between BS and UE is blocked by obstacles. In practical communication systems, if the direct link is not negligible, we can carry out the beam training between BS and UE individually by turning off the RIS and applying existing frameworks.

B. Conventional Beam Training Framework

Due to the severe path loss of THz communication systems, directional beams need to be generated by beamforming to achieve high array gain to compensate for the severe attenuation. Therefore, the CSI is crucial for accurate beamforming. Beam training is a near-optimal framework to acquire the CSI by estimating the best direction to transmit signals [18], [19], [20], [21]. Considering the fact that the locations of the BS and the RIS are fixed once deployed, the channel between BS and RIS has a much longer coherence time than that between RIS and UE, which can be treated as quasi-static [41]. Therefore, we suppose the channel $\mathbf{h}_{br,m}$ between BS and RIS is known perfectly by the BS and the purpose of beam training is converted into estimating the best beam direction between the RIS and the UE.

Traditional beam training framework [23] usually applies the DFT codebook with the beam training vectors being $\mathbf{v}_n = \mathrm{diag}\,(\mathbf{a}_N\,(\theta_n))$, where θ_n is distributed uniformly over the entire beam directions with $\theta_n = \frac{2n-N}{N}, n = 0, 1, \cdots, N - 1$. Specifically, the DFT codebook with size N can be represented by

$$\mathbf{W} = \left[\mathbf{a}_N(-1), \mathbf{a}_N\left(\tfrac{2-N}{N}\right), \cdots, \mathbf{a}_N\left(\tfrac{N-2}{N}\right) \right]$$

$$= \begin{bmatrix} 1 & 1 & \cdots & 1 \\ e^{-j\pi} & e^{j\frac{2-N}{N}\pi} & \cdots & e^{j\frac{N-2}{N}\pi} \\ \vdots & \vdots & \ddots & \vdots \\ e^{-jN\pi} & e^{jN\frac{2-N}{N}\pi} & \cdots & e^{jN\frac{N-2}{N}\pi} \end{bmatrix}. \tag{6}$$

During the beam training process, each column of $\mathbf{W}$ is applied for beamforming to transmit pilots in different time slots, and the UE can receive a series of pilots with the received power being $\mathbf{p} = [p_0, p_1, \cdots, p_{N-1}]$, where $p_n = |y_n|^2 = \left| \mathbf{h}_{ru,m}^H \mathrm{diag}\,(\mathbf{W}\,[:, n]) \mathbf{h}_{br,m} \right|^2$. The index i that

achieves the largest received power is given by

$$i = \underset{0 \le i < N}{\arg \max}\, p_i. \tag{7}$$

The best direction $\theta_i = \frac{2i-N}{N}$ can be decided accordingly. Then, the system can transmit data with the beamforming vector being $\mathbf{a}_N\left(\frac{2i-N}{N}\right)$.

The above beam training framework is based on the directional narrow beams achieved by DFT codewords. However, in RIS-assisted wideband THz communication systems, considering the frequency-independent phase shift of RIS, there exists the beam split effect, which means the spatial direction φ_m varies at different subcarriers. This effect will lead to the phenomenon that the beams at different subcarriers are steered to different physical directions. Specifically, for the beamforming vector $\mathbf{v}_n = \mathrm{diag}\,(\mathbf{a}_N\,(\theta_n))$, the beam at the m-th subcarrier is actually steered to $\theta_{n,m} = (f_c/f_m)\,\theta_n = \theta_n/\xi_m$. In this scenario, narrow beams with high angular resolution cannot be generated normally. As a consequence, conventional beam training frameworks, if directly applied in wideband systems, will experience severe performance degradation since the angular resolution of the designed beams is low. We can certainly carry out the beam training respectively for each subcarrier, but this will lead to an unacceptable beam training overhead and this method cannot exploit the information that could originally be carried in the frequency domain, which effaces the advantage of the large bandwidth of THz systems. Therefore, an accurate beam training framework for RIS-assisted wideband THz communication systems is needed.

III. PROPOSED ANALYTICAL BEAM TRAINING FRAMEWORK

In order to estimate the UE direction accurately in RIS-assisted wideband THz communication systems, in this section, we introduce the proposed analytical beam training framework. Specifically, we first give an overview of our proposed framework. Then, we elaborate the analysis of PDP and propose the PDP-based direction estimation scheme. Finally, based on the PDP-based direction estimation scheme, we design the analytical codebook according to the inherent parameter of the THz system for the proposed framework.

A. Overview of Proposed Analytical Beam Training Framework

Traditional beam training schemes only utilize the maximum received power to *choose* the best direction from a series of previously designed directions. This means that the accuracy of traditional beam training schemes depends heavily on the angular resolution of the generated beams. However, as mentioned above, in RIS-assisted wideband THz systems, generating beams with high angular resolution without extra hardware costs is impossible, so the beam training accuracy is limited. Luckily, the large bandwidth in THz systems actually carries more information in the frequency domain. The authors in [42] exploited the coupling between the freuqency and

radiation angle of leaky-wave antennas to determine the UE direction effectively. Although the structure and property of leaky-wave antennas are different from those of the RIS elements, this study provides us with the insight that the beam split effect can be a merit rather than a demerit for beam training.

Specifically, the beam split effect caused by the large bandwidth makes the received power of a certain beam at different directions in space vary in a particular pattern, which is called the power distribution pattern (PDP) in this paper. The PDP is caused by two aspects. For one thing, for each subcarrier, the beam gain near the beam center is the largest, while the beam gain near the edge of the beam gradually decreases, which causes the power to vary in a particular pattern. For another, due to the beam split effect in the system, the beams at different subcarriers will deviate from the central direction. The total power (i.e., the summation of power from all subcarriers) near the central direction will be the larger since a relatively greater number of subcarriers can transmit signals to this direction. However, the total power near the edge of the designed wide beam will be small since only the subcarriers with the lowest / highest frequency can transmit signals to these directions. If the PDP can be analyzed specifically, the direction of the UE can be derived according to the received power. Following this idea, we can take advantage of the PDP brought by the beam split effect in wideband THz systems to make this effect a benefit rather than a drawback.

In practice, the received power decreases as the distance between the UE and RIS increases, which leads to a lower SNR, so the absolute value of the received power is meaningless. We introduce a pair of beams with the same width and a ratio metric based on the respective received powers of the two beams. The two beams have the same beam width and are adjacent to each other. To eliminate the impacts of distances, a ratio metric based on the respective received powers of the two beams is also introduced. This ratio can normalize the received power to make itself unrelated to the distance. Additionally, this ratio and the direction in space are in one-to-one correspondence, which means that the UE direction can be analytically derived based on the received power of the beam pairs. The proposed analytical beam training framework can improve the accuracy of beam training, since we consider the beam split effect during the analysis of PDP and analytically calculate the best direction. In this way, the beam training accuracy is independent of the angular resolution of the generated beams.

Based on this, the proposed analytical beam training framework can be described as follows. The BS transmits training signals based on the proposed analytical codebook in different time slots. Then, the UE selects the beam pair which has the maximum normalized received power. Based on the exact value of the received power, the best direction can be analytically calculated based on the proposed PDP-based direction estimation scheme and then fed back to the BS, which is utilized for future data transmission. The specific process of the proposed analytical beam training framework is illustrated in **Algorithm 1**, which consists of three stages.

Algorithm 1 Proposed Analytical Beam Training Framework

Inputs: Analytical codebook $\mathbf{W}$, central directions of the beam pairs $\boldsymbol{\mu}$; power normalization coefficient $\boldsymbol{\zeta}$; beam training overhead P

Output: The estimated UE direction $\hat{\phi}$

1: **Training stage:**
2: **for** $i = 1$ to P **do**
3:     $\boldsymbol{\Theta} = \mathrm{diag}\left(\mathbf{W}\left[:, i\right]\right)$
4:     Transmit beam training signals based on the $\boldsymbol{\Theta}$ and save the received power as $\mathbf{p}\left[i\right]$
5: **end for**
6: **Calculating stage:**
7: $\tilde{\mathbf{p}} = \mathbf{p} \odot \boldsymbol{\zeta}$
8: Estimate the UE direction $\hat{\phi}$ by the PDP-based direction estimation scheme based on $\tilde{\mathbf{p}}$.
9: **Date transmission stage:**
10: Transmit data based on the estimated direction $\hat{\phi}$

Specifically, during the training stage, in the i-th time slot, the BS transmits training signal with the RIS configuration being $\boldsymbol{\Theta} = \mathrm{diag}\left(\mathbf{W}\left[:, i\right]\right)$, which is selected from the proposed analytical codebook $\mathbf{W}$. The UE saves the corresponding received power in each time slot in $\mathbf{p}$. After the time slots allocated for beam training are exhausted, the received power is normalized by the power normalization coefficient $\boldsymbol{\zeta}$. The reason for introducing the power normalization coefficient is that the beam widths of different beam pairs differ, which leads to the differences in the array gain since the total transmit power is fixed. Then, in the calculating stage, the beam pair which has the largest normalized received power $\tilde{\mathbf{p}}$ is chosen, based on which the UE direction can be directly calculated from the proposed PDP-based direction estimation scheme, which is elaborated in the next subsection. Finally, we transmit data according to the estimated direction in the data transmission stage.

In the following two subsections, we will introduce in detail the proposed PDP-based direction estimation scheme and the design of our proposed analytical codebook.

B. Proposed PDP-Based Direction Estimation

In this subsection, we first introduce the method to generate wide beams. Then, we analyze the PDP of the beam pair in wideband THz systems. Finally, based on the above analysis, we propose the PDP-based direction estimation scheme.

We first introduce the method that we apply to generate a wide beam. When generating traditional narrow beams, the beamforming matrices are designed as $\boldsymbol{\Theta} = \mathrm{diag}\left(\mathbf{a}_N\left(\theta\right)\right)$. The spatial width $W = 2/N$ is inversely proportional to the number of elements N on RIS. If N reduces, then the spatial width of the beam will naturally increase. Therefore, we follow the method in [43] where the RIS is divided into several sub-arrays, where the traditional beamforming method is applied to each of the sub-array. By organizing the direction of all the sub-arrays to let them cover the target directions, we can form a wide beam with the designed width.
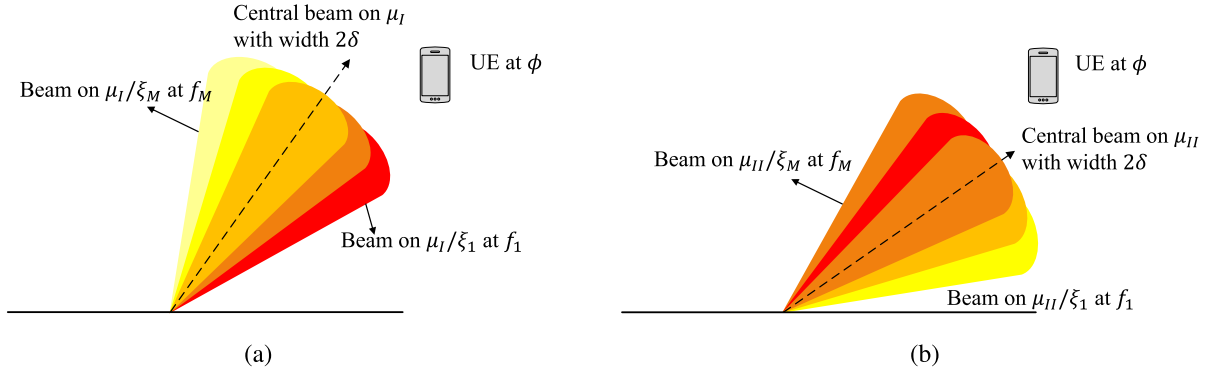
Fig. 2.   Received power of the beam pair (a) Beam I. (b) Beam II.

Specifically, we divide the RIS into K sub-arrays, which satisfies

$$\frac{2}{N_s} \times K \geq \varpi, \qquad (8)$$

where N_s is the number of antenna elements in each sub-array, and ϖ is the target width. Since K and N_s are two integers, we have $KN_s \leq N$, which means $K = \lfloor \frac{N}{N_s} \rfloor \geq \frac{N}{N_s} - 1$, so by substituting K with $\frac{N}{N_s} - 1$, we get a sufficient condition for (8) as

$$N_s \leq \frac{\sqrt{1 + 2N\varpi} - 1}{\varpi}. \qquad (9)$$

In order to achieve enough array gain to compensate for the serious path loss, we need N_s to be as large as possible so that the array gain of each sub-array is high enough. Due to the relaxation of K, the condition in (9) is not tight. Therefore, we need to increase the N_s until it cannot satisfy (8) to get the largest N_s, and K can be constrained as $K = \lfloor \frac{N}{N_s} \rfloor$.

After determining K and N_s, we need to specify the directions of beams generated by different sub-arrays to make them cover the target range. We denote the central direction of the designed wide beam as μ. Since the beam width of each sub-array is $2/N_s$, the direction of the k-th sub-array can be presented as

$$\nu_k = \mu + \frac{2k - K - 1}{N_s}, \quad k = 1, 2, \cdots, K. \qquad (10)$$

Therefore, the phase-shift matrix of RIS can be written as

$$\Theta[i(k,n), i(k,n)] = \frac{1}{\sqrt{N}} e^{j\pi[(k-1)N_s + n - 1]\nu_k} e^{j\epsilon_k},$$
$$k = 1, 2, \cdots, K + 1, n = 1, 2, \cdots, N_s, \qquad (11)$$

where $i(k,n) = (k-1)N_s + n$ denotes the index of the RIS units, and ϵ_k is the phase compensation in order to avoid the serration and guarantee enough array gain, which satisfies $\epsilon_k = k\Delta\epsilon$, where $\Delta\epsilon$ is presented as

$$\Delta\epsilon = \begin{cases} \dfrac{(N_s - 1)\pi}{N_s} + \pi, & N_s^4 \sin^2\left(\dfrac{\pi}{2N_s}\right) \geq 8, \\[3mm] 2\arccos\left(\dfrac{\sqrt{2}}{4}N_s^2 \sin\dfrac{\pi}{2N_s}\right), & N_s^4 \sin^2\left(\dfrac{\pi}{2N_s}\right) < 8. \end{cases} \qquad (12)$$

The derivation of ϵ_k is elaborated in **Appendix A**.

Based on the generation of the wide beam, we then analyze the beam gain of the sidelobe to prove the optimality of selecting the beam pair with the maximum received power for analysis. For each sub-array, the beamforming vector is conjugate to the array response vector, which makes the beam directed to a given angle. According to the **Lemma 1** in [44], the ratio of the gain of the sidelobe to the maximum beam gain η satisfies $\eta \leq \left(\frac{1}{N \sin \frac{3\pi}{2N}}\right)$, which increases with the increament of N, and η reaches its maximum when N reaches its minimum. Since $\varpi \leq 2$, $N_s \geq \sqrt{N}$. Taking the case $N = 1024$ as an example, then η satisfies $\eta < 0.213$. Accordingly, the maximum ratio of the received power of the sidelobe to the beam center is no more than 0.05. This property holds for all sub-arrays. Therefore, for the generated wide beam, the power of the sidelobe is much smaller than the power of the mainlobe, and thus can be neglected, which guarantees the optimality of selecting the beam pair with the maximum received power for analysis.

We consider a targeted UE at ϕ, where $\phi = \frac{c}{2df_m}\psi_m$ as defined in (3). For a wide beam steered to μ with width 2δ (both in spatial domain), and the subcarrier frequencies ranging from f_1 to f_M, the directions of beams at each subcarrier range from $\frac{\mu}{\xi_M}$ to $\frac{\mu}{\xi_1}$, where $\xi_m = f_m/f_c$. As a result, for the m_+-th subcarrier, where m_+ satisfies

$$m_+ \in \mathcal{M}_+ = \left\{ m \mid \frac{\mu}{\xi_m} - \delta \leq \phi \leq \frac{\mu}{\xi_m} + \delta, m \in \mathcal{M} \right\},$$
$$\mathcal{M} = \{1, 2, \ldots, M\}, \qquad (13)$$

the received power is greater than a threshold. While for the m_--th subcarrier, which satisfies

$$m_- \in \mathcal{M}_- = \left\{ m \mid \phi < \frac{\mu}{\xi_m} - \delta \parallel \phi > \frac{\mu}{\xi_m} + \delta, m \in \mathcal{M} \right\},$$
$$\mathcal{M} = \{1, 2, \cdots, M\}, \qquad (14)$$

the received power is less than this threshold. Therefore, while μ changes, the received power at UE changes, which carries the information of the physical direction of the UE. Actually, this is a kind of extra information compared to traditional beam training schemes. Existing beam training schemes mostly follow the idea of *choosing*, where the best physical direction with the maximum received power is chosen from a series of previously designed directions, so the accuracy of beam training depends on the angular resolution of generated beams. These schemes only utilize the
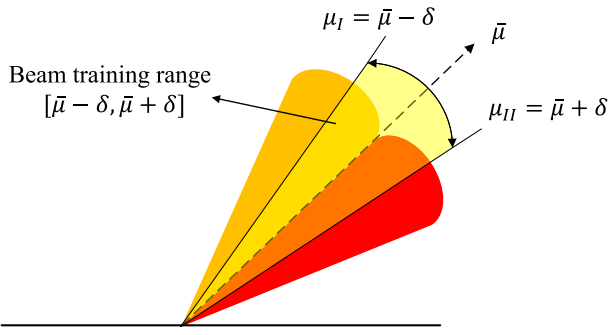
Fig. 3. Designed beam pair and the corresponding beam training range.

(a)

(b)

Fig. 4. (a) The PDP of a beam pair. (b) The relationship between χ and the estimated direction ϕ.

information of the relationship between the received powers, but the exact value of the received power has not been fully exploited. The above property allows us to take advantage of the exact values of the received power to improve the beam training accuracy in wideband THz communication systems.

We consider a pair of beams, as is illustrated in Fig. 2, for beam I, the received powers of subcarriers indexed by $m_{+,\mathrm{I}} \in \mathcal{M}_{+,\mathrm{I}} = \{m \mid \tilde{m} \le m \le M\}$ are greater than a threshold, while the received powers of subcarriers indexed by $m_{-,\mathrm{I}} \in \mathcal{M}_{-,\mathrm{I}} = \{m \mid 1 \le m < \tilde{m}\}$ are less than the threshold. For beam II, the received powers of subcarriers indexed by $m_{-,\mathrm{II}} \in \mathcal{M}_{-,\mathrm{II}} = \{m \mid 1 \le m < \tilde{m}\}$ are greater than a threshold, while the received powers of subcarriers indexed by $m_{+,\mathrm{II}} \in \mathcal{M}_{+,\mathrm{II}} = \{m \mid \tilde{m} \le m \le M\}$ are less than the threshold. This phenomenon results in the difference in the received power corresponding to the two beams at the UE. If we design the directions and widths of the beam pair appropriately, we can use the received power to analytically derive the physical direction of the UE.

Next, we analyze in detail the PDP of the beam pair. The PDP represents how the summation of beam powers from all subcarriers vary in space. As is illustrated in Fig. 3, we denote the central direction of the beam pair as $\bar{\mu}$. Since the estimation of the direction is based on the received power, the beam width of each beam pair needs to be the same so that their array gain will be the same, which is fair for further calculation. As is mentioned above, the beam steered to μ covers an angular range from $\frac{\mu}{\xi_M}$ to $\frac{\mu}{\xi_1}$. This is the direction range that carries the information brought by wide bandwidth.Therefore, we set the width of the beam pair as $\varpi = 2\delta = \bar{\mu}(f_c/f_1 - f_c/f_M) \approx \bar{\mu}B/f_c$. As for the central direction of each wide beam, we want to fully utilize the channel information carried by each subcarrier, so for the m-th subcarrier, if the received power is greater than the threshold at beam I, it should be less than the threshold at beam II, and vice versa.As a result, the difference in the central direction of the two wide beams should equal the beam width, which means $\mu_{\mathrm{I}} = \bar{\mu} - \delta$ and $\mu_{\mathrm{II}} = \bar{\mu} + \delta$. With this setting, UE in $[\bar{\mu} - \delta, \bar{\mu} + \delta]$ is able to receive the signals of both wide beams and the received power can be utilized to calculate the physical direction of this UE.
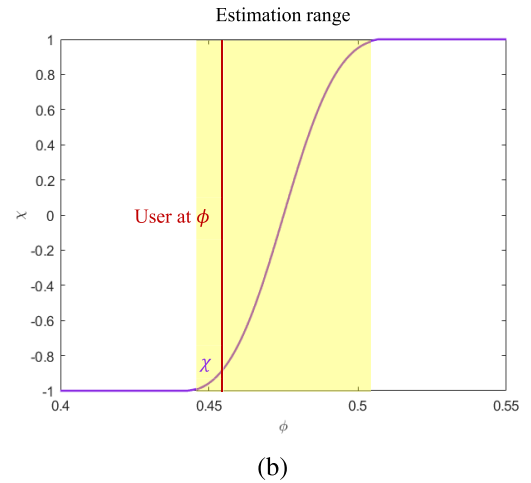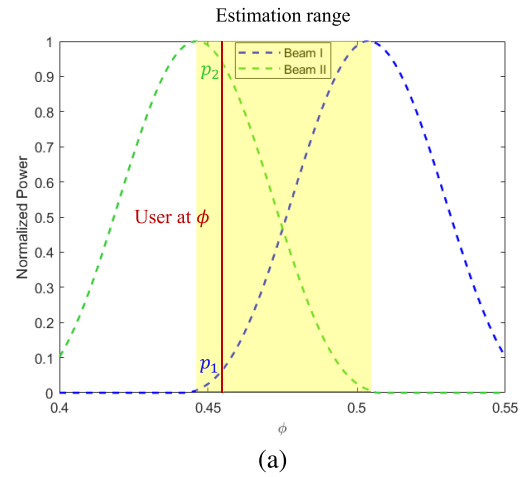
To analyze the PDP, we need to derive the power of a beam at an arbitrary angle in space. For a UE at $\phi \in [\bar{\mu} - \delta, \bar{\mu} + \delta]$, the PDP of beam I can be presented as

$$|g_{\mathrm{I}}(\phi)|^2 = \left| \sum_{m=1}^{M} \left[\mathbf{a}_N^H(\phi_m) \operatorname{diag}(\boldsymbol{\Theta}(\mu_{\mathrm{I}})) \right] \right|^2$$
$$\approx \mathcal{C} \frac{\sin^2\left(\frac{\pi N_s(\phi - \bar{\mu} + \delta)}{2}\right)}{\sin^2\left(\frac{\pi(\phi - \bar{\mu} + \delta)}{2}\right)}, \quad (15)$$

where $\phi_m = \frac{f_c}{f_m}\phi$, $\mathcal{C}$ is a constant independent of ϕ and μ_{I}. The derivation of (15) is elaborated in **Appendix B**.

Similarly, for the same UE at $\phi \in [\bar{\mu} - \delta, \bar{\mu} + \delta]$, the PDP of beam II can be presented as

$$|g_{\mathrm{II}}(\phi)|^2 \approx \mathcal{C} \frac{\sin^2\left(\frac{\pi N_s(\phi - \bar{\mu} - \delta)}{2}\right)}{\sin^2\left(\frac{\pi(\phi - \bar{\mu} - \delta)}{2}\right)}, \quad (16)$$

where $\mathcal{C}$ is a constant independent of ϕ and μ_{II}. Since $\delta \approx K/N_s$ according to (8), the numerators of (15) and (16) equal to each other, thus the difference of received power relies on the denominators.

Based on the received power of the beam pair, we then introduce the proposed PDP-based direction estimation scheme.

As illustrated in Fig. 4(a), the highlighted region represents the angle range that this beam pair can accurately estimate. It can be observed that the received power of the two beams within the estimation range is unique, so for a certain UE at ϕ, the relationship between p_1 and p_2 can be utilized to derive the UE direction.

Considering the random noise and the unknown transmitting distance, the absolute value of the received power itself is meaningless. In order to obtain the direction estimator, we need to choose the appropriate metric. For a certain beam pair, the relative difference of these two received powers eliminates the uncertain factors in the system and carries the actual information of the channel. Therefore, we introduce the ratio metric $\chi = \chi(\phi)$ as

$$\chi(\phi) = \frac{|g_{\mathrm{I}}(\phi)|^2 - |g_{\mathrm{II}}(\phi)|^2}{|g_{\mathrm{I}}(\phi)|^2 + |g_{\mathrm{II}}(\phi)|^2}. \tag{17}$$

By applying (15) and (16), χ can be re-written as

$$
\begin{aligned}
\chi(\phi) &= \frac{\sin^2\left(\frac{\pi(\phi-\bar{\mu}-\delta)}{2}\right) - \sin^2\left(\frac{\pi(\phi-\bar{\mu}+\delta)}{2}\right)}{\sin^2\left(\frac{\pi(\phi-\bar{\mu}-\delta)}{2}\right) + \sin^2\left(\frac{\pi(\phi-\bar{\mu}+\delta)}{2}\right)} \\
&= -\frac{\sin(\pi(\phi-\bar{\mu}))\sin(\pi\delta)}{1 - \cos(\pi(\phi-\bar{\mu}))\cos(\pi\delta)},
\end{aligned} \tag{18}
$$

where $\phi - \bar{\mu} \in [-\delta, \delta]$. The estimation of direction ϕ can then be explicitly acquired by inverting the function $\chi(\cdot)$, i.e.,

$$\hat{\phi} = \bar{\mu} - \arcsin\left(\frac{\chi\sin(\pi\delta) - \chi\sqrt{1-\chi^2}\sin(\pi\delta)\cos(\pi\delta)}{\sin^2(\pi\delta) + \chi^2\cos^2(\pi\delta)}\right). \tag{19}$$

The relationship between the UE direction and the ratio metric χ is demonstrated in Fig. 4(b), showing that χ and ϕ are in one-to-one correspondence. Therefore, based on (19), we can estimate the direction ϕ of UE.

Compared with traditional beam training schemes based on *choosing* the best direction, the proposed PDP-based direction estimation scheme considers the beam split effect in wideband THz systems and analytically *calculate* the UE direction based on the PDP of the beam pair, which makes full use of the information that is carried in the frequency domain and makes the beam split effect an advantage rather than a drawback. Therefore, the proposed scheme improves the accuracy of beam training since the beam split effect is considered during derivation. In addition, the above derivation is also adaptive to traditional narrowband systems and can improve the beam training accuracy in narrowband systems. However, when the bandwidth is small, the beam split effect no longer exists, which means that the estimation ranges of the beam pairs are small. As a result, the proposed scheme will suffer from a large beam training overhead (i.e., proportional to the number of RIS elements) in narrowband systems. As a result, the proposed framework is more practical in wideband THz systems.

C. Design of the Proposed Analytical Codebook

Based on the above derivation, we introduce the analytical codebook design in RIS-assisted wideband THz communi-

cation systems. The codebook design can be divided into two steps. The first step is to design the codeword for the directions where the beam split effect is very weak, which can be neglected. For this part, using traditional beam training codebooks is enough. The second step is to design the codeword for the directions where our proposed analytical beam training framework works well. The framework on how to design the codebook is summarized in **Algorithm 2**.

Algorithm 2 Proposed Analytical Codebook Design

Inputs: Number of units on RIS N; bandwidth B, central frequency f_c; range parameter κ; dividing parameter β

Outputs: Central directions of the beam pairs $\boldsymbol{\mu}$; estimation range $\boldsymbol{\rho}$; power normalization coefficient $\boldsymbol{\zeta}$; designed analytical codebook $\mathbf{W}$

1: **Initialization:**
   $\boldsymbol{\mu} = \left[-\frac{1}{N}, \frac{1}{N}\right]$; $\boldsymbol{\rho} = \left[-\frac{1}{N}, \frac{1}{N}\right]$; $\boldsymbol{\zeta} = \left[\frac{2}{N}, \frac{2}{N}\right]$;

2: **while** $B\boldsymbol{\mu}[0]/f_c > -\beta$ **do**

3: $\quad \boldsymbol{\mu} = \left[\boldsymbol{\mu}[0] - \frac{2}{N}, \boldsymbol{\mu}, -\boldsymbol{\mu}[0] + \frac{2}{N}\right]$;

4: $\quad \boldsymbol{\rho} = \left[\boldsymbol{\rho}[0] - \frac{2}{N}, \boldsymbol{\rho}, -\boldsymbol{\rho}[0] + \frac{2}{N}\right]$;

5: $\quad \boldsymbol{\zeta} = \left[\frac{2}{N}, \boldsymbol{\zeta}, \frac{2}{N}\right]$;

6: **end while**

7: **while** $\boldsymbol{\rho}[0] > -1$ **do**

8: $\quad \bar{\mu} = -\frac{2\boldsymbol{\rho}[0]f_c}{2f_c - \kappa B}$;

9: $\quad \delta = \frac{B}{2f_c}\bar{\mu}$;

10: $\quad \boldsymbol{\mu} = [-\bar{\mu}, \boldsymbol{\mu}, \bar{\mu}]$;

11: $\quad \boldsymbol{\rho} = [-\bar{\mu} - \kappa\delta, \boldsymbol{\rho}, \bar{\mu} + \kappa\delta]$;

12: $\quad \boldsymbol{\zeta} = \left[\frac{B\bar{\mu}}{f_c}, \boldsymbol{\zeta}, \frac{B\bar{\mu}}{f_c}\right]$;

13: **end while**

14: Generate the codebook $\mathbf{W}$ by Eq. (11) based on $\boldsymbol{\mu}$

15: **return** $\boldsymbol{\mu}, \boldsymbol{\rho}, \boldsymbol{\zeta}, \mathbf{W}$

Specifically, we need to generate the central direction of the beam pairs $\boldsymbol{\mu}$, the estimation range $\boldsymbol{\rho}$ and the power normalization coefficient $\boldsymbol{\zeta}$ for beam training, based on which we generate the analytical codebook. During the generation process, we first introduce a dividing parameter β to divide the directions where the beam split effect can be neglected and the directions where the beam split effect is serious. For the first part, we utilize traditional narrow beams to estimate the optimal direction, so the difference in central direction is $2/N$. Traditionally, the directions of narrow beams are equivalent to the estimation range, so $\boldsymbol{\rho}$ is equal to $\boldsymbol{\mu}$ in this part, and the power normalization coefficient $\boldsymbol{\zeta}$ is equal to the width of the generated narrow beams. For the second part where the beam split effect is serious, we introduce the range parameter κ. According to (19), as is illustrated in Fig. 4(b), for a pair of designed wide beams, although we can theoretically estimate the direction in range $[\bar{\mu} - \delta, \bar{\mu} + \delta]$, the gradient near the boundary is approximately 0, which means a slight difference in χ will result in a large deviation of ϕ.

In practical communication systems, there exist various kinds of noise, which is inevitable, so we need to introduce the range parameter $0 < \kappa < 1$ to limit the estimation range in $[\bar{\mu} - \kappa\delta, \bar{\mu} + \kappa\delta]$ to improve the accuracy of estimation.

Based on the previous estimation range $\bar{\mu} + \kappa\delta$, the central direction of the next beam pair should satisfy

$$\bar{\mu}_{new} - \kappa\frac{B}{2f_c}\bar{\mu}_{new} = \bar{\mu}_{old} + \kappa\frac{B}{2f_c}\bar{\mu}_{old} = -\boldsymbol{\rho}\,[0]\,,$$

$$\Longrightarrow \bar{\mu}_{new} = -\frac{2\boldsymbol{\rho}\,[0]\,f_c}{2f_c - \kappa B}. \qquad (20)$$

Then, the central direction of the next wide beam is determined. We can extend the codebook until the estimation range can cover all directions $[-1, 1]$ in space. It is worth noting that the array gains of the different wide beams are different because the total transmission powers are fixed but the width of wide beams vary. Therefore, we need to generate a power normalization coefficient for each wide beam, whose value is proportional to the beam width. After getting the received power of each codeword $\mathbf{p}$, we get the normalized received power by $\tilde{\mathbf{p}} = \mathbf{p} \odot \boldsymbol{\zeta}$. By choosing the maximum element in $\tilde{\mathbf{p}}$, we can determine which pair of wide beams can estimate the direction of this user. Then the estimated direction $\hat{\phi}$ can be obtained by (19). It can be observed from the process of designing the analytical codebook that the size of the proposed analytical codebook is related only to the inherent system parameters such as the central frequency and the bandwidth, which makes it highly adaptive to future communication systems with massive antenna elements.

IV. EXTENSIONS OF THE PROPOSED ANALYTICAL BEAM TRAINING FRAMEWORK

In this section, we discuss the extension of the proposed analytical beam training framework to different scenarios. Firstly, we extend the proposed framework to multi-user scenarios. Then, the scenarios where the BS and the UE are equipped with antenna arrays are discussed. Finally, we extend the proposed framework to the scenarios where the RIS is a uniform planar array (UPA).

A. Extension to Multi-User Scenarios

Similar to the existing multi-directional schemes, the proposed framework is also applicable for multi-user scenarios since the calculation stage can be conducted independently at different UEs. Specifically, in the training stage, the BS still transmits beam training signals based on the designed analytical codebook $\boldsymbol{\Theta}$ sequentially. At this stage, all users in the communication system can simultaneously receive the signals and record the received powers. Then, at the calculation stage, the entire calculation process is conducted at each user based on the pre-recorded received powers and the proposed PDP-based direction estimation scheme independently. After the calculation, the direction of multiple users are fed back to the BS and RIS for the future data transmission stage.

B. Extension to MIMO Scenarios

To make the main idea of the proposed framework more clear, we assume that the BS and UE are equipped with a single antenna in the above sections. In THz systems, considering the high path loss of THz signals, it is more practical to deploy antenna arrays at the BS or the UE. In this subsection, we elaborate on how to extend the proposed framework to the scenarios where the BS or the UE are equipped with antenna arrays.

When the BS is equipped with an N_t-element ULA, the downlink channel at the m-th subcarrier between the BS and the RIS $\mathbf{h}_{br,m} \in \mathbb{C}^{N \times N_t}$ with $m = 1, 2, \cdots, M$ can be denoted as

$$\mathbf{h}_{br,m} = g_{br,m}e^{-j2\pi\tau_{br,m}f_m}\mathbf{a}_N(\varphi_m)\mathbf{a}_{N_t}^T(\vartheta_m), \qquad (21)$$

where $\mathbf{a}_{N_t}(\vartheta)$ represents the array response associated to the BS and ϑ_m represents the spatial angle of the BS. Accordingly, the received signal y_m at the m-th subcarrier at the UE can be presented as

$$y_m = \mathbf{h}_{ru,m}^H \boldsymbol{\Theta} \mathbf{h}_{br,m} \mathbf{A} s_m + n_m, \qquad (22)$$

where $\mathbf{A} \in \mathbb{C}^{N_t \times 1}$ denotes the precoding matrix at the BS. As stated in Section II-B, considering the quasi-static property of the BS-RIS channel, we suppose that the channel $\mathbf{h}_{br,m}$ between the BS and RIS is known by the system. The precoding matrix at the BS $\mathbf{A}$ can then be designed to compensate for the high path loss of THz signals, which is also known by the system. Therefore, (22) can be converted to (5) by substituting $\mathbf{h}_{br,m}$ in (5) by $\tilde{\mathbf{h}}_{br,m} = \mathbf{h}_{br,m}\mathbf{A}$ in (22). The problem of estimating the UE direction when the BS is equipped with an N_t-element ULA is thus converted to the single-antenna case that is already solved above.

When the UE is equipped with an N_r-element ULA, the downlink channel at the m-th subcarrier between the RIS and the UE $\mathbf{h}_{ru,m} \in \mathbb{C}^{N \times N_r}$ with $m = 1, 2, \cdots, M$ can be denoted as

$$\mathbf{h}_{ru,m} = g_{ru,m}e^{-j2\pi\tau_{ru,m}f_m}\mathbf{a}_N(\psi_m)\mathbf{a}_{N_r}^T(\omega_m), \qquad (23)$$

where $\mathbf{a}_{N_r}$ represents the array response associated to the UE and ω_m represents the spatial angle of the UE. Accordingly, the received signal y_m at the m-th subcarrier can be presented as

$$\mathbf{y}_m = \mathbf{h}_{ru,m}^H \boldsymbol{\Theta} \mathbf{h}_{br,m} s_m + \mathbf{n}_m, \qquad (24)$$

where $\mathbf{y}_m \in \mathbb{C}^{N_r \times 1}$ represents the received signals at each antenna of UE. In this case, the proposed framework can still work if we analyze the received signals of each antenna respectively or the summation of the received powers at all antennas.

C. Extensions to UPA Scenarios

The proposed framework can be extended to the scenarios where the RIS is a uniform planar array (UPA). In the UPA RIS system, both the azimuth angle and the elevation angle of the UE need to be estimated. We consider the compact allocated reflecting elements on the UPA RIS with $N = N_1 \times N_2$ elements, where the antenna spacing $d = \iota\frac{\lambda_c}{2} < \frac{\lambda_c}{2}$ [45]. Accordingly, the array response vector should be modified as

$$\mathbf{b}_N(\phi_p, \theta_p) = \frac{1}{\sqrt{N}}\left[e^{-j\pi\frac{2d}{c}f_m\sin(\theta_p)\sin(\phi_p)\mathbf{n}_1}\right]$$
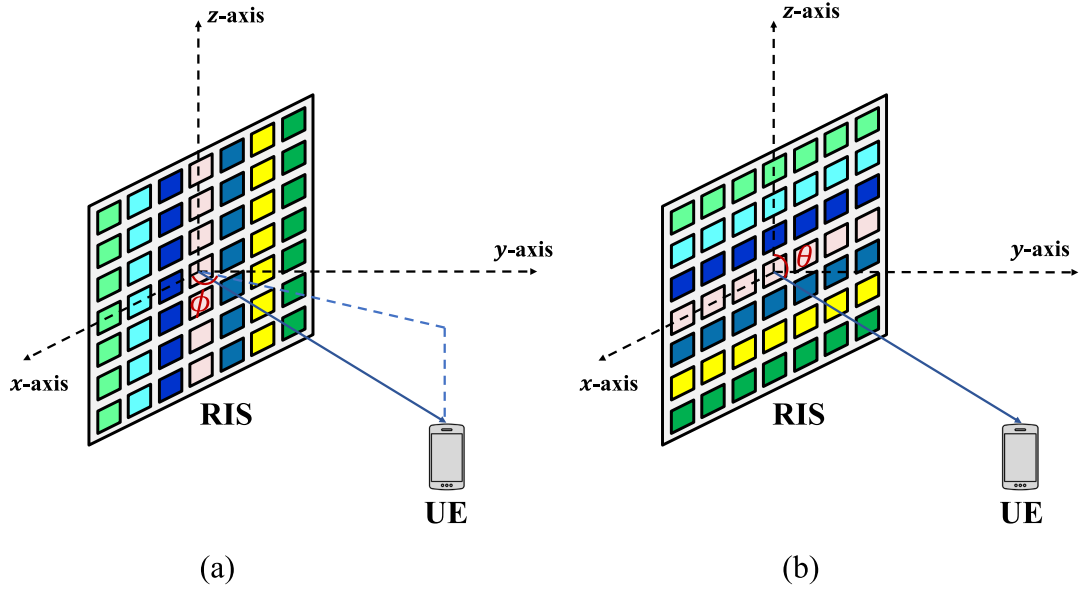
Fig. 5. The extension of the proposed scheme to UPA RIS: (a) Estimate $\sin(\theta_p)\sin(\phi_p)$ of UE; (b) Estimate $\cos(\theta_p)$ of UE.

$$\otimes \left[e^{-j\pi \frac{2d}{c} f_m \cos(\theta_p) \mathbf{n}_2} \right], \quad (25)$$

where $\mathbf{n}_1 = [0, 1, \cdots, N_1 - 1]$, $\mathbf{n}_2 = [0, 1, \cdots, N_2 - 1]$, θ_p and ϕ_p denote the physical elevation angle and the physical azimuth angle, respectively. We can observe from (25) that the array response vector of the UPA is composed of two parts. The first part is related to $\sin(\theta_p)\sin(\phi_p)$ while the second part is related to $\cos(\theta_p)$, and the two part is corresponding to the rows of elements on the UPA and the columns of elements on the UPA, respectively. To extend the proposed scheme to UPA RIS, we can conduct the proposed PDP-based direction estiamtion scheme twice to sequentially estimate $\sin(\theta_p)\sin(\phi_p)$ and $\cos(\theta_p)$.

Specifically, as illustrated in Fig. 5 (a), we firstly estimate $\sin(\theta_p)\sin(\phi_p)$. We can set the reflecting coefficients of the elements at the same column as the same. The reflecting matrix of the UPA RIS can be presented as $\boldsymbol{\Theta}_{\text{UPA}} = \text{diag}(\mathbf{w} \otimes \frac{1}{\sqrt{N_2}} \mathbf{1}_{N_2 \times 1})$, where $\mathbf{w}$ represents a certain codeword in the designed analytical codebook $\mathbf{W}$ and $\mathbf{1}_{N_2 \times 1}$ represents an all-one vector with size $N_2 \times 1$. Then, the array gain at the m-th subcarrier can be derived as

$$\left| \mathbf{b}_N(\phi_p, \theta_p) \text{diag}^{-1}(\boldsymbol{\Theta}) \right|^2$$

$$= \left| \frac{1}{\sqrt{N_1}} \left[e^{-j\pi \frac{2d}{c} f_m \sin(\theta)\sin(\phi) \mathbf{n}_1} \right] \mathbf{w} \right.$$
$$\otimes \left. \frac{1}{N_2} \left[e^{-j\pi \frac{2d}{c} f_m \cos(\theta_p) \mathbf{n}_2} \right] \mathbf{1}_{N_2 \times 1} \right|^2$$
$$= \left| \frac{1}{\sqrt{N_1}} \left[e^{-j\pi \iota \frac{f_m}{f_c} \sin(\theta_p)\sin(\phi_p) \mathbf{n}_1} \right] \mathbf{w} \right.$$
$$\otimes \left. \frac{1}{N_2} \sum_{n=1}^{N_2} e^{-j\pi \iota \frac{f_m}{f_c} \cos(\theta_p)(n-1)} \right|^2. \quad (26)$$

By adding up the received powers at all subcarriers, the received power of a certain codeword can be derived as (27), shown at the bottom of the page, where (a) $\sim$ (c) are approximated similarly as **Appendix B**. According to (27), the difference between the UPA case and the ULA case is that the array gain is related not only to $\sin(\theta_p)\sin(\phi_p)$ that we aim to estimate, but also to $\cos(\theta_p)$. However, for a certain user located at (ϕ_p, θ_p), the last term in (27) is also a constant. Therefore, the PDP of the UPA case is still the same as that of the ULA case and $\sin(\theta_p)\sin(\phi_p)$ can then be estimated. Similarly, $\cos(\theta_p)$ can be estimated as illustrated in Fig. 5 (b). We set the reflecting coefficients of the elements at the same row as the same. The reflecting matrix of the UPA RIS can be

$$|g(\phi)|^2 \overset{(a)}{\approx} \frac{1}{N^2} \sum_{m=1}^{M} \left| \sum_{n_{s1}=1}^{N_{s1}} e^{j\pi(n_{s1}-1)(\iota \frac{f_m}{f_c} \sin(\theta_p)\sin(\phi_p) - \bar{\mu} + \delta)} \sum_{n_2=1}^{N_2} e^{-j\pi \iota \frac{f_m}{f_c} \cos(\theta_p)(n_2-1)} \right|^2$$

$$\overset{(b)}{\approx} \frac{1}{N^2} \sum_{m=1}^{M} \left| \frac{\sin(\frac{N_{s1}\pi}{2}(\iota \frac{f_m}{f_c} \sin(\theta_p)\sin(\phi_p) - \bar{\mu} + \delta))}{N_{s1} \sin(\frac{\pi}{2}(\iota \frac{f_m}{f_c} \sin(\theta_p)\sin(\phi_p) - \bar{\mu} + \delta))} \frac{\sin(\frac{N_2\pi}{2} \iota \frac{f_m}{f_c} \cos(\theta_p))}{N_2 \sin(\frac{\pi}{2}(\iota \frac{f_m}{f_c} \cos(\theta_p)))} \right|^2$$

$$\overset{(c)}{\approx} \mathcal{C} \frac{\sin^2\left(\frac{\pi N_{s1}(\iota \sin(\theta_p)\sin(\phi_p) - \bar{\mu} + \delta)}{2}\right)}{\sin^2\left(\frac{\pi(\iota \sin(\theta_p)\sin(\phi_p) - \bar{\mu} + \delta)}{2}\right)} \frac{\sin^2\left(\frac{\pi N_2(\iota \cos(\theta_p))}{2}\right)}{\sin^2\left(\frac{\pi(\iota \cos(\theta_p))}{2}\right)}. \quad (27)$$
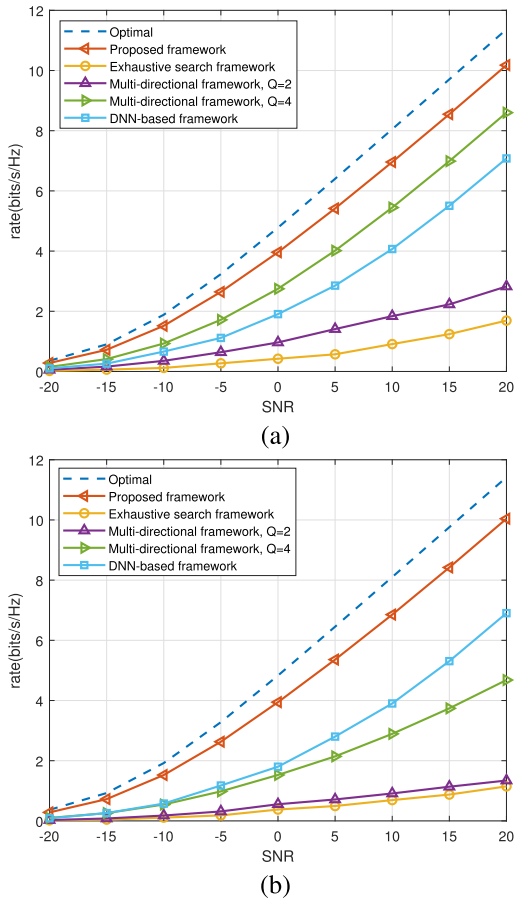
Fig. 6. The achievable rate performance v.s. the SNR. The number of elements of RIS is set to (a) 1024, (b) 2048.

Fig. 7. The achievable rate performance v.s. the beam training overhead. The number of elements of RIS is set to (a) 1024, (b) 2048.

presented as $\boldsymbol{\Theta}_{\mathrm{UPA}} = \mathrm{diag}(\frac{1}{\sqrt{N_1}}\mathbf{1}_{N_1 \times 1} \otimes \mathbf{w})$. Then, the PDP can be derived similarly as (26) and (27), and the $\cos(\theta)$ can then be estimated.

V. SIMULATION RESULTS

In this section, simulation results are provided to verify the performance of the proposed analytical beam training framework. The parameters of the RIS-assisted wideband THz communication system are set to $N_{\mathrm{BS}} = 1$, $N_{\mathrm{UE}} = 1$, $f_c = 100$ GHz, $B = 10$ GHz, the number of subcarriers is set to 128. The UE direction is set to satisfy $\phi \sim \mathcal{U}\left(-\frac{\sqrt{3}}{2}, \frac{\sqrt{3}}{2}\right)$. The proposed framework is compared with the multi-directional framework in [28], the DNN-based framework in [29] and the exhaustive search framework, since these three schemes do not need frequent interactions between the UE and BS/RIS.

Fig. 6 illustrates the achievable rate performance v.s. the SNR. The achievable rate is calculated as

$$R = \frac{1}{M} \sum_{m=1}^{M} \log 2 \left(1 + \frac{P_t}{\sigma^2} \mathbf{h}_{ru,m}^H \boldsymbol{\Theta} \mathbf{h}_{br,m} \mathbf{h}_{br,m}^H \boldsymbol{\Theta}^H \mathbf{h}_{ru,m}\right), \tag{28}$$

where P_t denotes the transmission power at the BS and σ^2 denotes the noise power. The reflecting vector $\boldsymbol{\Theta}$ is obtained based on the space-time block coding-based beamforming scheme in [46] so that all subcarriers can transmit signals
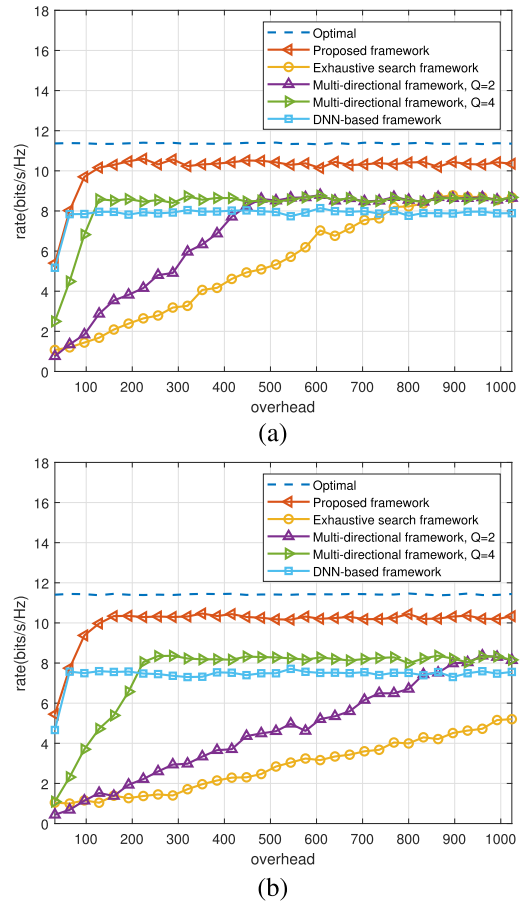
to the UE with the presence of the beam split effect. Here we set the training overhead to 128. The parameter Q in the multi-directional beam training framework represents the number of beam directions in each time slot. The SNR (the ratio of the received signal power to the received noise power) increases from -20 dB to 20 dB to evaluate the performance of the proposed framework in both the high SNR scenarios and the low SNR scenarios. In Fig. 6(a), the number of RIS elements is 1024, we can observe that the data-driven scheme achieves a worse achievable rate performance than the multi-directional scheme since the beam training overhead is sufficient for multi-directional scheme. In Fig. 6(b), the data-driven scheme achieves a better achievable rate performance than multi-directional scheme since the beam training overhead is no longer sufficient for multi-directional schemes with the increament of the number of RIS elements. On the contrary, the data-driven scheme, benefiting from a low beam training overhead, can achieve a similar achievable rate performance with the case when $N_{\mathrm{RIS}} = 1024$. However, the existing schemes all neglect the beam split effect in the wideband THz systems. As a result, our proposed analytical beam training scheme possesses the best achievable rate performance in both cases.

Fig. 7 illustrates the rate performance of different frameworks as the training overhead increases. Here the SNR is set to 20 dB. The x-axis represents the beam training overhead.
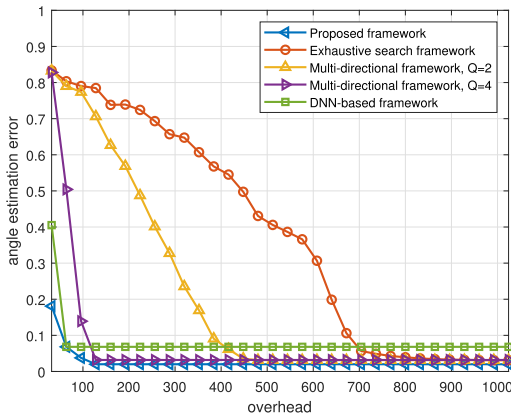
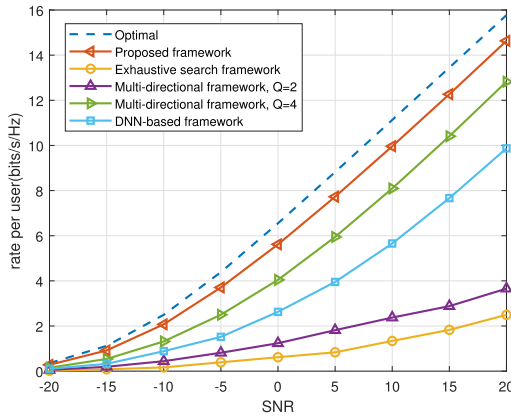Fig. 8. The angle estimation error v.s. the beam training overhead.

Fig. 9. The achievable rate performance of each user v.s. the SNR when the BS is a 128×1 ULA.
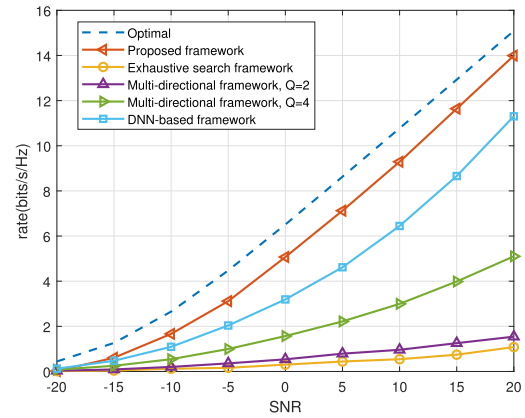

Fig. 10. The achievable rate performance v.s. the SNR when the RIS is a 64×64 UPA.
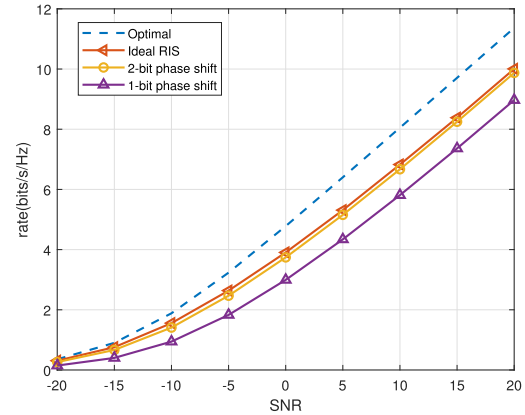
Fig. 11. The achievable rate performance v.s. the SNR with quantized phase shifts.

The beam training overhead is increasing from 32 to 1024. We can observe from Fig. 7 that the proposed analytical beam training framework can achieve near-optimal achievable rate performance and outperforms the existing frameworks no matter how high the beam training overhead is. It is worth noting that when the training overhead is limited (the scanned angles are limited), the achievable rate performance is much better than the existing frameworks. This is because our proposed framework can significantly reduce the training overhead when the UE is far from $0°$ where the beam split effect is severe. By scanning the space from $90°/-90°$ to $0°$, we can accurately estimate a large proportion of directions with a very low training overhead.

To intuitively reveal the beam training accuracy, we compare the angle estimation error of different schemes v.s. the beam training overhead in Fig. 8. The beam training SNR is set to 20 dB. The number of RIS elements is 1024. The beam training overhead increases from 32 to 1024. It is illustrated that the proposed framework can realize the estimation with the lowest estimation error with a low beam training overhead since the beam split effect is exploited. The angle estimation error of the multi-directional frameworks and the exhaustive search framework is a little higher than the proposed framework since the beam split effect leads to a lower the angular resolution. The DNN-based framework, despite the low beam training overhead, has the worst angle estimation performance.

We extend the proposed framework to the multi-user scenarios, where the BS is equipped with a 128×1 ULA. The beam training overhead is set to 128. The SNR is increasing from -20 dB to 20 dB. It can be observed from Fig. 9 that the proposed beam training scheme can still reach the near-optimal achievable rate performance for each user. The existing schemes, however, suffer from a performance loss with the presence of the beam split effect.

We also compare the achievable rate performance v.s. the SNR when the RIS is a $64 \times 64 = 4096$ UPA in Fig. 10. The beam training overhead is set to 256. When the number of RIS elements increases, the beam training overhead for multi-directional frameworks is not sufficient, which leads to a low achievable rate. The DNN-based framework, benefiting from the low beam training overhead, can reach a higher achievable rate. Since the beam split effect is taken into consideration, our proposed scheme can still reach the highest achievable rate.

Considering the hardware limitation of the phase shifters, we also demonstrate how the limited RIS quantization bit may affect the performance of the proposed framework in Fig. 11. We compare the achievable rate performance of the proposed framework when the phase shifts of the RIS elements are consecutive (Ideal RIS), quantized with 2-bit and quantized with 1-bit. The number of RIS elements is 1024. The beam training overhead is set to 128. The SNR

is increasing from -20 dB to 20 dB. We quantize the phase shift of the RIS according to the nearest neighbour criterion. We can observe from Fig. 11 that when the RIS quantization bit is 2-bit, the proposed framework realizes nearly the same achievable rate performance as the ideal RIS case. When the RIS quantization bit is 1-bit, the achievable rate performance only decreases 10%, which verifies the effectiveness of the proposed framework in systems with hardware limitations.

To sum up, the proposed analytical beam training framework can reach the near-optimal achievable rate performance with a low training overhead as long as there exists beam split effect in the system, and can be easily extended to multiple scenarios.

VI. CONCLUSION

In this paper, we investigated the beam training problem in RIS-assisted wideband THz communication systems. We proposed an analytical beam training framework to improve the beam training accuracy in wideband communication systems,. Specifically, we first analyzed the PDP of the beam pair in RIS-assisted wideband THz systems and proposed a PDP-based direction estimation scheme, which converted the traditional idea of *choosing* the best direction to the new idea of analytically *calculating* the best direction. Based on this scheme, we designed an analytical codebook for the proposed analytical beam training framework according to the inherent parameters of the THz systems. Since the proposed framework considered the beam split effect in wideband communication systems and took full advantage of the relative values of the received power, it could improve the beam training accuracy in future communication systems. Simulation results showed that the proposed framework outperformed the existing beam training framework and can obtain the near-optimal achievable rate performance with a low beam training overhead. For future works, we will further investigate the beam training problem in wideband near-field scenarios.

APPENDIX A
DERIVATION OF THE PHASE COMPENSATION IN (11)

The array gain of the k-th sub-array at $\bar{\nu}$ can be presented as

$$
|g(k)|^2
$$
$$
= \left| \mathbf{a}_N^H (\bar{\nu}) \operatorname{diag}^{-1} (\mathbf{\Theta} (\nu_k)) \right|^2
$$
$$
= \left| \sum_{p=1}^{K+1} \sum_{n=1}^{N_s} \frac{1}{N} e^{-j\pi[(p-1)N_s+n-1]\bar{\nu}} e^{j\pi[(p-1)N_s+n-1]\nu_k} e^{j\epsilon_p} \right|^2
$$
$$
= \frac{1}{N^2} \left| \sum_{p=1}^{K+1} e^{-j\pi(p-1)(2p-2k-1)} e^{j\epsilon_p} \sum_{n=1}^{N_s} e^{j\pi(n-1)\frac{2p-2k-1}{N_s}} \right|^2
$$
$$
\overset{(a)}{\approx} \frac{1}{N^2} \left| e^{j\pi(k-1)} e^{j\epsilon_k} \sum_{n=1}^{N_s} e^{\frac{-j\pi(n-1)}{N_s}} \right.
$$

$$
\left. + e^{-j\pi k} e^{j\epsilon_{k+1}} \sum_{n=1}^{N_s} e^{\frac{j\pi(n-1)}{N_s}} \right|^2
$$
$$
= \frac{1}{N^2} \left| \sum_{n=1}^{N_s} e^{\frac{-j\pi(n-1)}{N_s}} - e^{j(\epsilon_{k+1}-\epsilon_k)} \sum_{n=1}^{N_s} e^{\frac{j\pi(n-1)}{N_s}} \right|^2
$$
$$
= \frac{1}{N^2} \frac{1}{N_s^2 \sin^2 \frac{\pi}{2N_s}} \left| e^{j\frac{(N_s-1)\pi}{2N_s}} - e^{j(\epsilon_{k+1}-\epsilon_k)} e^{-j\frac{(N_s-1)\pi}{2N_s}} \right|^2,
$$
(29)

where (a) is explained by **Lemma 1**.

Lemma 1:

$$
\left| \sum_{p=1}^{K+1} \sum_{n=1}^{N_s} e^{j\pi(n-1)\frac{2p-2k-1}{N_s}} \right|^2
$$
$$
\approx \left| \sum_{n=1}^{N_s} e^{-j\pi\frac{n-1}{N_s}} + \sum_{n=1}^{N_s} e^{j\pi\frac{n-1}{N_s}} \right|^2. \quad (30)
$$

Proof:

$$
\left| \sum_{p=1}^{K+1} \sum_{n=1}^{N_s} e^{j\pi(n-1)\frac{2p-2k-1}{N_s}} \right|^2
$$
$$
= \left| \sum_{p=1}^{K+1} e^{j\pi\frac{2k-2p+1}{N_s}} \frac{\sin \frac{N_s\pi}{2}\frac{2p-2k-1}{N_s}}{N_s \sin \frac{\pi}{2}\frac{2p-2k-1}{N_s}} e^{j\frac{(3N_s-1)\pi}{2}\frac{2p-2k-1}{N_s}} \right|^2.
$$
(31)

We consider the value of $f(p) = \left| \frac{\sin \frac{N_s\pi}{2}\frac{2p-2k-1}{N_s}}{N_s \sin \frac{\pi}{2}\frac{2p-2k-1}{N_s}} \right|^2, p = 1, 2, \cdots, K+1$, due to the symmetry of this function, when $p = k+1/2$, $f(p)$ reaches its maximum value 1. However, since p is an integer, the actual maximum value of $f(p)$ is reached when $p^* = k$ and $p^* = k+1$. If p is not the two maximum points above, we have

$$
\frac{f(p)}{f(p^*)} \leq \frac{\sin^2 \pi/2N_s}{\sin^2 3\pi/2N_s}, \quad (32)
$$

where N_s is relatively large, so we have $\frac{f(p)}{f(p^*)} \leq 1/9$, thus these terms can be neglected. By reserving the two maximum points of $f(p)$, the lemma can be proved. ∎

According to (29), the total array gain at $\bar{\nu}$ can be presented as

$$
\mathcal{P} = |g(k)|^2 + |g(k+1)|^2
$$
$$
= \mathcal{C} \left(\left| e^{j\frac{(N_s-1)\pi}{2N_s}} - e^{j(\epsilon_{k+1}-\epsilon_k)} e^{-j\frac{(N_s-1)\pi}{2N_s}} \right|^2 \right.
$$
$$
\left. + \left| e^{j\frac{(N_s-1)\pi}{2N_s}} - e^{j(\epsilon_{k+2}-\epsilon_{k+1})} e^{-j\frac{(N_s-1)\pi}{2N_s}} \right|^2 \right), \quad (33)
$$

where $\mathcal{C} = \frac{1}{N^2 N_s^2 \sin^2 \frac{\pi}{2N_s}}$ is a constant independent of ϵ. It is easy to see that the two terms have the same structure, in order to avoid the serration and guarantee enough array gain, we set

$\mathcal{P} = N_s^2/N^2$, which is the designed array gain of each sub-array, thus we have

$$\left| e^{j\frac{(N_s-1)\pi}{2N_s}} - e^{j(\epsilon_{k+1}-\epsilon_k)} \, e^{-j\frac{(N_s-1)\pi}{2N_s}} \right|^2$$

$$= \min \left\{ 4, \frac{N_s^4 \sin^2\left(\frac{\pi}{2N_s}\right)}{2} \right\}. \quad (34)$$

For simplicity, we only derive the equation for the first term, due to the same structure, the equation for the second term is similar as (34). Therefore, the phase compansation ϵ must satisfies

$$\Delta\epsilon = \begin{cases} \dfrac{(N_s-1)\pi}{N_s} + \pi & N_s^4 \sin^2\left(\dfrac{\pi}{2N_s}\right) \geq 8 \\[2ex] 2\arccos\left(\dfrac{\sqrt{2}}{4} N_s^2 \sin\dfrac{\pi}{2N_s}\right) & N_s^4 \sin^2\left(\dfrac{\pi}{2N_s}\right) < 8, \end{cases}$$
$$(35)$$

where $\Delta\epsilon = \epsilon_{k+1} - \epsilon_k$ for all $k = 1, 2, \cdots, K$. We might as well set ϵ as $\epsilon_k = k\Delta\epsilon$. Thus the phase-shift matrix of RIS can be obtained by (10), (11) and (35).

APPENDIX B
DERIVATION OF (15)

$$|g(\phi)|^2 = \sum_{m=1}^{M} \left| \sum_{k=1}^{K+1} \sum_{n=1}^{N_s} \frac{1}{\sqrt{N}} e^{-j\pi[(k-1)N_s+n-1]\phi_m} \right.$$

$$\left. \frac{1}{\sqrt{N}} e^{j\pi[(k-1)N_s+n-1]\nu_k} e^{j\epsilon_k} \right|^2$$

$$= \frac{1}{N^2} \sum_{m=1}^{M} \left| \sum_{k=1}^{K+1} e^{-j\pi(k-1)N_s(\phi_m-\nu_k)} \right.$$

$$\left. e^{j\epsilon_k} \sum_{n=1}^{N_s} e^{j\pi(n-1)(\phi_m-\nu_k)} \right|^2. \quad (36)$$

According to **Lemma 1**, the expression can further be approximated as

$$|g(\phi)|^2$$
$$\approx \frac{1}{N^2}$$
$$\times \sum_{m=1}^{M} \left| \underbrace{e^{-j\pi(k_1-1)N_s(\phi_m-\nu_{k_1})} e^{j\epsilon_{k_1}}}_{(a)} \sum_{n=1}^{N_s} e^{j\pi(n-1)(\phi_m-\nu_{k_1})} \right.$$

$$\left. + \underbrace{e^{-j\pi(k_2-1)N_s(\phi_m-\nu_{k_2})} e^{j\epsilon_{k_2}}}_{(b)} \sum_{n=1}^{N_s} e^{j\pi(n-1)(\phi_m-\nu_{k_2})} \right|^2,$$
$$(37)$$

where $k_1 = \lfloor \frac{(\phi_m-\bar{\mu}+\delta)N_s+K+1}{2} \rfloor$, $k_2 = \lceil \frac{(\phi_m-\bar{\mu}+\delta)N_s+K+1}{2} \rceil$. Here, (a) and (b) are the phase compensation, so the two items

can be merged. Therefore, we have

$$|g(\phi)|^2 \approx \frac{1}{N^2} \sum_{m=1}^{M} \left| e^{-j\pi\epsilon_1} \sum_{n=1}^{N_s} e^{j\pi(n-1)(\phi_m-\bar{\mu}+\delta)} \right|^2$$

$$= \frac{1}{N^2} \sum_{m=1}^{M} \left| \frac{\sin\left(\frac{N_s\pi}{2}(\phi_m-\bar{\mu}+\delta)\right)}{N_s \sin\left(\frac{\pi}{2}(\phi_m-\bar{\mu}+\delta)\right)} \right.$$

$$\left. e^{j\frac{(N_s-1)\pi}{2}(\phi_m-\bar{\mu}+\delta)} \right|^2$$

$$\approx \mathcal{C} \frac{\sin^2\left(\frac{\pi N_s(\phi-\bar{\mu}+\delta)}{2}\right)}{\sin^2\left(\frac{\pi(\phi-\bar{\mu}+\delta)}{2}\right)}. \quad (38)$$

REFERENCES

[1] I. F. Akyildiz, J. M. Jornet, and C. Han, "Terahertz band: Next frontier for wireless communications," *Phys. Commun.*, vol. 12, pp. 16–32, Sep. 2014.

[2] T. S. Rappaport et al., "Wireless communications and applications above 100 GHz: Opportunities and challenges for 6G and beyond," *IEEE Access*, vol. 7, pp. 78729–78757, 2019.

[3] Z. Zhang et al., "6G wireless networks: Vision, requirements, architecture, and key technologies," *IEEE Veh. Technol. Mag.*, vol. 14, no. 3, pp. 28–41, Sep. 2019.

[4] M. Giordani, M. Polese, M. Mezzavilla, S. Rangan, and M. Zorzi, "Toward 6G networks: Use cases and technologies," *IEEE Commun. Mag.*, vol. 58, no. 3, pp. 55–61, Mar. 2020.

[5] C. Han, A. O. Bicen, and I. F. Akyildiz, "Multi-wideband waveform design for distance-adaptive wireless communications in the terahertz band," *IEEE Trans. Signal Process.*, vol. 64, no. 4, pp. 910–922, Feb. 2016.

[6] Q. Wu and R. Zhang, "Towards smart and reconfigurable environment: Intelligent reflecting surface aided wireless network," *IEEE Commun. Mag.*, vol. 58, no. 1, pp. 106–112, Jan. 2020.

[7] Q. Wu and R. Zhang, "Intelligent reflecting surface enhanced wireless network via joint active and passive beamforming," *IEEE Trans. Wireless Commun.*, vol. 18, no. 11, pp. 5394–5409, Nov. 2019.

[8] E. Basar, M. Di Renzo, J. De Rosny, M. Debbah, M.-S. Alouini, and R. Zhang, "Wireless communications through reconfigurable intelligent surfaces," *IEEE Access*, vol. 7, pp. 116753–116773, 2019.

[9] S. Dash, C. Liaskos, I. F. Akyildiz, and A. Pitsillides, "Wideband perfect absorption polarization insensitive reconfigurable graphene metasurface for THz wireless environment," in *Proc. IEEE Microw. Theory Techn. Wireless Commun. (MTTW)*, vol. 1, Oct. 2019, pp. 93–96.

[10] Z. Zhang and L. Dai, "Reconfigurable intelligent surfaces for 6G: Nine fundamental issues and one critical problem," *Tsinghua Sci. Technol.*, vol. 28, no. 5, pp. 929–939, Oct. 2023.

[11] Y. Zhao et al., "High-speed efficient terahertz modulation based on tunable collective-individual state conversion within an active 3 nm two-dimensional electron gas metasurface," *Nano Lett.*, vol. 19, no. 11, pp. 7588–7597, Nov. 2019.

[12] S. Venkatesh, X. Lu, H. Saeidi, and K. Sengupta, "A high-speed programmable and scalable terahertz holographic metasurface based on tiled CMOS chips," *Nature Electron.*, vol. 3, no. 12, pp. 785–793, Dec. 2020.

[13] C. You, B. Zheng, and R. Zhang, "Channel estimation and passive beamforming for intelligent reflecting surface: Discrete phase shift and progressive refinement," *IEEE J. Sel. Areas Commun.*, vol. 38, no. 11, pp. 2604–2620, Nov. 2020.

[14] S. Ma, W. Shen, J. An, and L. Hanzo, "Wideband channel estimation for IRS-aided systems in the face of beam squint," *IEEE Trans. Wireless Commun.*, vol. 20, no. 10, pp. 6240–6253, Oct. 2021.

[15] C. Huang et al., "Multi-hop RIS-empowered terahertz communications: A DRL-based hybrid beamforming design," *IEEE J. Sel. Areas Commun.*, vol. 39, no. 6, pp. 1663–1677, Jun. 2021.

[16] D. Tyrovolas, S. A. Tegos, E. C. Dimitriadou-Panidou, P. D. Diamantoulakis, C. K. Liaskos, and G. K. Karagiannidis, "Performance analysis of cascaded reconfigurable intelligent surface networks," *IEEE Wireless Commun. Lett.*, vol. 11, no. 9, pp. 1855–1859, Sep. 2022.

[17] L. Dai et al., "Reconfigurable intelligent surface-based wireless communications: Antenna design, prototyping, and experimental results," *IEEE Access*, vol. 8, pp. 45913–45923, 2020.

[18] W. Wu, D. Liu, X. Hou, and M. Liu, "Low-complexity beam training for 5G millimeter-wave massive MIMO systems," *IEEE Trans. Veh. Technol.*, vol. 69, no. 1, pp. 361–376, Jan. 2020.

[19] A. Ali, N. González-Prelcic, and R. W. Heath, "Millimeter wave beam-selection using out-of-band spatial information," *IEEE Trans. Wireless Commun.*, vol. 17, no. 2, pp. 1038–1052, Feb. 2018.

[20] X. Gao, L. Dai, Z. Chen, Z. Wang, and Z. Zhang, "Near-optimal beam selection for beamspace mmWave massive MIMO systems," *IEEE Commun. Lett.*, vol. 20, no. 5, pp. 1054–1057, May 2016.

[21] C. You, B. Zheng, and R. Zhang, "Fast beam training for IRS-assisted multiuser communications," *IEEE Wireless Commun. Lett.*, vol. 9, no. 11, pp. 1845–1849, Nov. 2020.

[22] R. Piesiewicz et al., "Short-range ultra-broadband terahertz communications: Concepts and perspectives," *IEEE Antennas Propag. Mag.*, vol. 49, no. 6, pp. 24–39, Dec. 2007.

[23] J. Suh, C. Kim, W. Sung, J. So, and S. W. Heo, "Construction of a generalized DFT codebook using channel-adaptive parameters," *IEEE Commun. Lett.*, vol. 21, no. 1, pp. 196–199, Jan. 2017.

[24] J. Wang et al., "Beam codebook based beamforming protocol for multi-Gbps millimeter-wave WPAN systems," *IEEE J. Sel. Areas Commun.*, vol. 27, no. 8, pp. 1390–1399, Oct. 2009.

[25] Z. Xiao, T. He, P. Xia, and X.-G. Xia, "Hierarchical codebook design for beamforming training in millimeter-wave communication," *IEEE Trans. Wireless Commun.*, vol. 15, no. 5, pp. 3380–3392, May 2016.

[26] H. Yu, P. Guan, W. Qu, and Y. Zhao, "An improved beam training scheme under hierarchical codebook," *IEEE Access*, vol. 8, pp. 53627–53635, 2020.

[27] B. Ning, Z. Chen, W. Chen, Y. Du, and J. Fang, "Terahertz multi-user massive MIMO with intelligent reflecting surface: Beam training and hybrid beamforming," *IEEE Trans. Veh. Technol.*, vol. 70, no. 2, pp. 1376–1393, Feb. 2021.

[28] P. Wang, J. Fang, W. Zhang, and H. Li, "Fast beam training and alignment for IRS-assisted millimeter wave/terahertz systems," *IEEE Trans. Wireless Commun.*, vol. 21, no. 4, pp. 2710–2724, Apr. 2022.

[29] C. Qi, Y. Wang, and G. Y. Li, "Deep learning for beam training in millimeter wave massive MIMO systems," *IEEE Trans. Wireless Commun.*, early access, Sep. 22, 2020, doi: 10.1109/TWC.2020.3024279.

[30] W. Liu, C. Pan, H. Ren, F. Shu, S. Jin, and J. Wang, "Low-overhead beam training scheme for extremely large-scale RIS in near field," *IEEE Trans. Commun.*, vol. 71, no. 8, pp. 4924–4940, Aug. 2023.

[31] B. Wang et al., "Spatial-wideband effect in massive MIMO with application in mmWave systems," *IEEE Commun. Mag.*, vol. 56, no. 12, pp. 134–141, Dec. 2018.

[32] V. Manev, M. Neofytou, G. Radulov, and K. Doris, "A novel analysis of the beam squinting in wideband phased array digital I/Q transmitters," in *Proc. Eur. Conf. Circuit Theory Design (ECCTD)*, Sep. 2020, pp. 1–4.

[33] X. Mo, W. Ma, L. Gui, L. Zhang, and X. Sang, "Beamspace channel estimation with beam squint effect for the millimeter-wave MIMO-OFDM systems," *IEEE Access*, vol. 9, pp. 153037–153049, 2021.

[34] J. Tan and L. Dai, "Delay-phase precoding for THz massive MIMO with beam split," in *Proc. IEEE Global Commun. Conf. (GLOBECOM)*, Dec. 2019, pp. 1–6.

[35] I. Mondal and N. Krishnapura, "A 2-GHz bandwidth, 0.25–1.7 ns true-time-delay element using a variable-order all-pass filter architecture in 0.13 μm CMOS," *IEEE J. Solid-State Circuits*, vol. 52, no. 8, pp. 2180–2193, Aug. 2017.

[36] C. Lin, G. Y. Li, and L. Wang, "Subarray-based coordinated beamforming training for mmWave and sub-THz communications," *IEEE J. Sel. Areas Commun.*, vol. 35, no. 9, pp. 2115–2126, Sep. 2017.

[37] E. Ghaderi, A. Sivadhasan Ramani, A. A. Rahimi, D. Heo, S. Shekhar, and S. Gupta, "An integrated discrete-time delay-compensating technique for large-array beamformers," *IEEE Trans. Circuits Syst. I, Reg. Papers*, vol. 66, no. 9, pp. 3296–3306, Sep. 2019.

[38] V. Boljanovic, H. Yan, E. Ghaderi, D. Heo, S. Gupta, and D. Cabric, "Design of millimeter-wave single-shot beam training for true-time-delay array," in *Proc. IEEE 21st Int. Workshop Signal Process. Adv. Wireless Commun. (SPAWC)*, May 2020, pp. 1–5.

[39] L. You, X. Gao, G. Y. Li, X.-G. Xia, and N. Ma, "BDMA for millimeter-wave/terahertz massive MIMO transmission with per-beam synchronization," *IEEE J. Sel. Areas Commun.*, vol. 35, no. 7, pp. 1550–1563, Jul. 2017.

[40] Y. Liu et al., "Reconfigurable intelligent surfaces: Principles and opportunities," *IEEE Commun. Surveys Tuts.*, vol. 23, no. 3, pp. 1546–1577, 3rd Quart., 2021.

[41] C. Hu, L. Dai, S. Han, and X. Wang, "Two-timescale channel estimation for reconfigurable intelligent surface aided wireless communications," *IEEE Trans. Commun.*, vol. 69, no. 11, pp. 7736–7747, Nov. 2021.

[42] Y. Ghasempour, R. Shrestha, A. Charous, E. Knightly, and D. M. Mittleman, "Single-shot link discovery for terahertz wireless networks," *Nature Commun.*, vol. 11, no. 1, p. 2017, Apr. 2020.

[43] L. Zhu, J. Zhang, Z. Xiao, X. Cao, D. O. Wu, and X.-G. Xia, "3-D beamforming for flexible coverage in millimeter-wave UAV communications," *IEEE Wireless Commun. Lett.*, vol. 8, no. 3, pp. 837–840, Jun. 2019.

[44] L. Dai, J. Tan, Z. Chen, and H. V. Poor, "Delay-phase precoding for wideband THz massive MIMO," *IEEE Trans. Wireless Commun.*, vol. 21, no. 9, pp. 7271–7286, Sep. 2022.

[45] D. Tyrovolas, S. A. Tegos, P. D. Diamantoulakis, and G. K. Karagiannidis, "Synergetic UAV-RIS communication with highly directional transmission," *IEEE Wireless Commun. Lett.*, vol. 11, no. 3, pp. 583–587, Mar. 2022.

[46] X. Liu and D. Qiao, "Space-time block coding-based beamforming for beam squint compensation," *IEEE Wireless Commun. Lett.*, vol. 8, no. 1, pp. 241–244, Feb. 2019.

Yuhao Chen (Graduate Student Member, IEEE) received the B.E. degree in electronic engineering from Tsinghua University, Beijing, China, in 2021, where he is currently pursuing the M.S. degree in electronic engineering. His research interests include massive MIMO, reconfigurable intelligent surface (RIS), and near-field communications. He received the IEEE ICC Outstanding Demo Award in 2022.

Jingbo Tan (Member, IEEE) received the B.S. and Ph.D. degrees from the Department of Electronic Engineering, Tsinghua University, Beijing, China, in 2017 and 2022, respectively. He is currently a Post-Doctoral Research Associate with Tsinghua University. His research interests include pre-coding and channel estimation in massive MIMO, THz communications, and reconfigurable intelligent surface aided systems. He has received the IEEE COMMUNICATIONS LETTERS Exemplary Reviewer Award in 2018, the Honorary Mention in the 2019 IEEE ComSoC Student Competition, the Outstanding Doctoral Dissertation of Tsinghua University in 2022, and the Beijing Outstanding Graduates in 2022.

Mo Hao received the bachelor's degree in electronic engineering from Sichuan University, China, in 2006, and the M.Sc. degree in microelectronic system design from Southampton University, U.K., in 2007. He was a Senior Engineer with Ericsson. He joined Tsinghua University as a Researcher in 2015. He is in charge of B5G related researches and project management. His research interests include massive MIMO, RIS, and other key technologies for beyond 5G.

Richard MacKenzie received the M.Eng. degree in electronic engineering from the University of York, York, U.K., and the Ph.D. degree in electronic engineering from the University of Leeds, Leeds, U.K.

Since 2009, he has been a Researcher of wireless communications with BT, where he is currently a Distinguished Engineer. His earlier work covered spectrum management, cognitive radio, femtocells, and next-generation technologies. He has involved in EU Projects, in particular QoSMOS, where he was a Work Package Leader of the network architecture design. He was a Spectrum Manager of the London 2012 Olympic and Paralympic Games. He was also part of BT's Bidding Team for spectrum auctions, notably the U.K. 4G spectrum auction in 2013, where BT re-entered the mobile market. He continues to research next-generation technologies, where his focus is to create an ecosystem for RAN virtualization, network automation, and the use of small cells. He is also a Technical Representative of BT, with many industry fora, including Telecom Infra Project (TIP), Next Generation Mobile Networks (NGMN), where he was the Chair of the RAN Functional Split and X-Haul Group and the O-RAN Alliance and Small Cell Forum. In TIP, he is the Co-Chair of the RAN Intelligence and Automation (RIA) OpenRAN Sub-Project.

Linglong Dai (Fellow, IEEE) received the B.S. degree from Zhejiang University, Hangzhou, China, in 2003, the M.S. degree (Hons.) from the China Academy of Telecommunications Technology, Beijing, China, in 2006, and the Ph.D. degree (Hons.) from Tsinghua University, Beijing, in 2011. From 2011 to 2013, he was a Post-Doctoral Research Fellow with the Department of Electronic Engineering, Tsinghua University, where he was an Assistant Professor (2013–2016), an Associate Professor (2016–2022), and a Professor (since 2022). His current research interests include massive MIMO, reconfigurable intelligent surface (RIS), millimeter-wave and terahertz communications, near-field communications, machine learning for wireless communications, and electromagnetic information theory. He has coauthored the book *MmWave Massive MIMO: A Paradigm for 5G* (Academic Press, 2016). He has authored or coauthored over 90 IEEE journal articles and over 50 IEEE conference papers. He also holds over 20 granted patents.

He has received five IEEE Best Paper Awards at IEEE ICC 2013, IEEE ICC 2014, IEEE ICC 2017, IEEE VTC 2017-Fall, and IEEE ICC 2018. He has also received the Tsinghua University Outstanding Ph.D. Graduate Award in 2011, the Beijing Excellent Doctoral Dissertation Award in 2012, the China National Excellent Doctoral Dissertation Nomination Award in 2013, the URSI Young Scientist Award in 2014, the IEEE TRANSACTIONS ON BROADCASTING Best Paper Award in 2015, the *Electronics Letters* Best Paper Award in 2016, the National Natural Science Foundation of China for Outstanding Young Scholars in 2017, the IEEE ComSoc Asia–Pacific Outstanding Young Researcher Award in 2017, the IEEE ComSoc Asia–Pacific Outstanding Paper Award in 2018, the *China Communications* Best Paper Award in 2019, the IEEE ACCESS Best Multimedia Award in 2020, the IEEE Communications Society Leonard G. Abraham Prize in 2020, the IEEE ComSoc Stephen O. Rice Prize in 2022, the IEEE ICC Outstanding Demo Award in 2022, and the National Science Foundation for Distinguished Young Scholars in 2023. He was listed as a Highly Cited Researcher by Clarivate Analytics, from 2020 to 2022.